Title

Techno-economic analysis of waste-heat conversion

Journal

Joule, 5(12)

ISSN

2542-4785

Authors

Geffroy, Charles
Lilley, Drew
Parez, Pedro Sanchez
et al.

Publication Date

2021-12-01

DOI

10.1016/j.joule.2021.10.014

Peer reviewed

Techno-economic analysis of waste-heat conversion

Charles Geffroy[1,$], Drew Lilley[1,2,$], Pedro Sanchez Parez[3], Ravi Prasher[1,2,*]
[1]Lawrence Berkeley National Laboratory, Berkeley, CA 94720, USA
[2]Department of Mechanical Engineering, University of California, Berkeley, CA 94720, USA
[3]Department of Mechanical Engineering, University of California, Merced, CA 95343, USA

[$]Equal contribution
*Corresponding author: rsprasher@lbl.gov

Summary

With more than 50% of the primary energy consumed worldwide currently lost as waste heat, waste-heat conversion (WHC) should be considered a promising zero-carbon source of electricity. Despite significant research on WHC, the market penetration of such technologies remains limited, in large part because the R&D community has primarily focused on the development of new WHC heat engines with limited attention given to the techno-economic aspects. As different types of WHC heat engines vary significantly in their physical origins, there is a critical need to develop a system-level techno-economic model that is relatively independent of the detailed physics and design of the engine. In this perspective, we develop a techno-economic model for WHC technologies based on the well-known endoreversible thermodynamics formulations, which results in a fairly universal model. Our results indicate that regardless of the type or efficiency, WHC heat engines are not economically viable below 100 °C, which has been the focus of significant research in the literature in recent years. Under highly optimistic assumptions such as the cost of the WHC heat engines is same as gas turbines (~$0.25/W) and the capacity factor of the waste heat source is 0.9, for relative device Carnot efficiency <0.2, which is typical of various WHC heat engines, WHC is economical only for temperatures above 150 °C and power output in the range of 100 kW to 1 MW. We conclude this perspective by providing a future outlook on the research needed in the field of WHC heat engines for it to be techno-economically viable. We also propose that along with the temperature and amount of waste heat available from various sources, the capacity factor of the waste heat sources must be documented.

Introduction

The use of waste heat and low-grade heat has fascinated scientists, engineers, and society as a whole for many decades[1,2]. The reason is very simple. Out of the ~475 EJ annual primary

energy consumption worldwide, ~50% is lost as waste heat[3]. Figure SI1 in the supplementary information (SI) shows the distribution of waste heat as a function of temperature for various energy sectors[3]. 156 EJ of this waste heat (or ~63% of the total available waste heat) is at low temperature[3] (<100 °C). Therefore there is tremendous interest specifically in the use of low-temperature waste heat[4–11]. The advent of nanostructured thermoelectrics in the early 2000s[12] led to a resurgence of interest in waste-heat utilization and particularly in the conversion of waste heat into electricity. Waste-heat conversion (WHC) into electricity -- also known as waste heat to power systems—is a potential technology[13,14] that can provide zero carbon electricity. Although thermoelectrics dominated[15] the early research because of its promise as a solid-state device with no moving parts and its modularity compared with traditional mechanical rotary-turbine-based technologies such as organic Rankine cycle (ORC) systems, many new non-rotary ideas have emerged in the past decade. Such is the interest in this topic that almost every year top science and engineering journals publish papers on new types of waste heat conversion engines[6–11]. What makes the WHC research very fascinating and interesting is that possibilities to use different physical phenomena are enormous. Examples include thermomagnetic generators[6], liquid-state thermocells[7], ionic heat-to-electricity conversion systems[10], electrochemical–thermal systems[11], and thermo-osmotic systems[8]. Potential applications are found in buildings, industry, transportation, and energy sectors, wherein waste heat is available at various temperatures – as shown in Fig. SI1.

However, despite such major scientific advancement and application potential, none of these technologies, including thermoelectrics, have penetrated the market or are able to compete in a scalable manner with traditional turbine-based technologies such as ORC. Table (1) shows a list of various types of heat engines, including their relative Carnot efficiency and temperature of operation. The effect of the irreversibility of engines is typically reported as the relative Carnot efficiency (ϕ) given by the ratio of device efficiency to the Carnot efficiency. Note that the relative Carnot efficiency shown in Table 1 is due to the internal irreversibility of the heat engine and does not include the irreversibility due to the heat exchangers. Table 1 shows that there are many options being explored for WHC below 100 °C. WHC below $100°C$ is an active area of research, commonly justified by the abundance of waste heat below 100 °C (Fig. SI1). Table 1 also shows that turbine-based ORC has high relative Carnot efficiency as compared to non-rotary heat engines which has a significant impact on economics of WHC as discussed later.

Heat Engine Technology	Relative Carnot Efficiency, ϕ, [%]	Operating Temperature Range (°C)
Liquid-state thermocells[7], thermomagnetic[6], thermo-osmotic[8], electrochemical–thermal[16], ionic heat-to-electricity conversion systems[10], thermogalvanic[17], pyroelectric[18],Thermoelectric[19]	<20	<100
Thermoelectric[19], Pyroelectric[20]	10 – 20	>100
High temperature electrochemical[21]	30	>500
Organic Rankine Cycle (ORC) [22]	50 – 90	>100

Table 1: A brief overview of the performance of various heat engines proposed in the literature for waste heat conversion. Relative Carnot efficiency is due to the internal irreversibility of the heat engine and does not include the irreversibility due to the heat exchangers. The relative Carnot efficiency is for the case of maximum power output (see text for details). Note that this list is meant to be illustrative and not exhaustive.

The R&D community has primarily focused on the technical optimization of heat-conversion devices (Fig. 1a) in an ideal lab setting without paying much attention to the thermal systems based on these technologies. One of the most important aspects not addressed in previous studies on novel/new heat engines is the impact of heat exchangers (required to get the heat in and out in any practical system) on the overall efficiency and cost of the system (Fig. 1b). Unlike turbine based traditional WHC technologies such as ORC[23,24], techno-economic analysis (TEA) models and cost targets for novel WHC heat engines have received little to no attention. The only exception is thermoelectrics where Yee et al. [25] developed a TEA model using various assumptions. Yee et al. were able to develop a TEA model for thermoelectrics because thermoelectrics have a long history and are commercially available for some applications. However the physics of novel heat engines can vary significantly as discussed in the examples in

Table 1 and detailed information are not available for novel heat engines. Thus, it is important to develop a TEA model which is to a large extent independent of the detailed physics of the system and is dependent mainly on known technological parameters, such as the temperature of the waste heat source, cost of heat exchangers, and expected irreversibility in the proposed heat engine. This type of TEA model will help in defining conditions and cost targets under which these novel WHC technologies can compete with other zero-carbon technologies such as solar PV- or ORC-based WHC/geothermal systems. This type of model will help tremendously in decision-making regarding the commercial viability as well as the overall impact of the design in solving the energy problem.

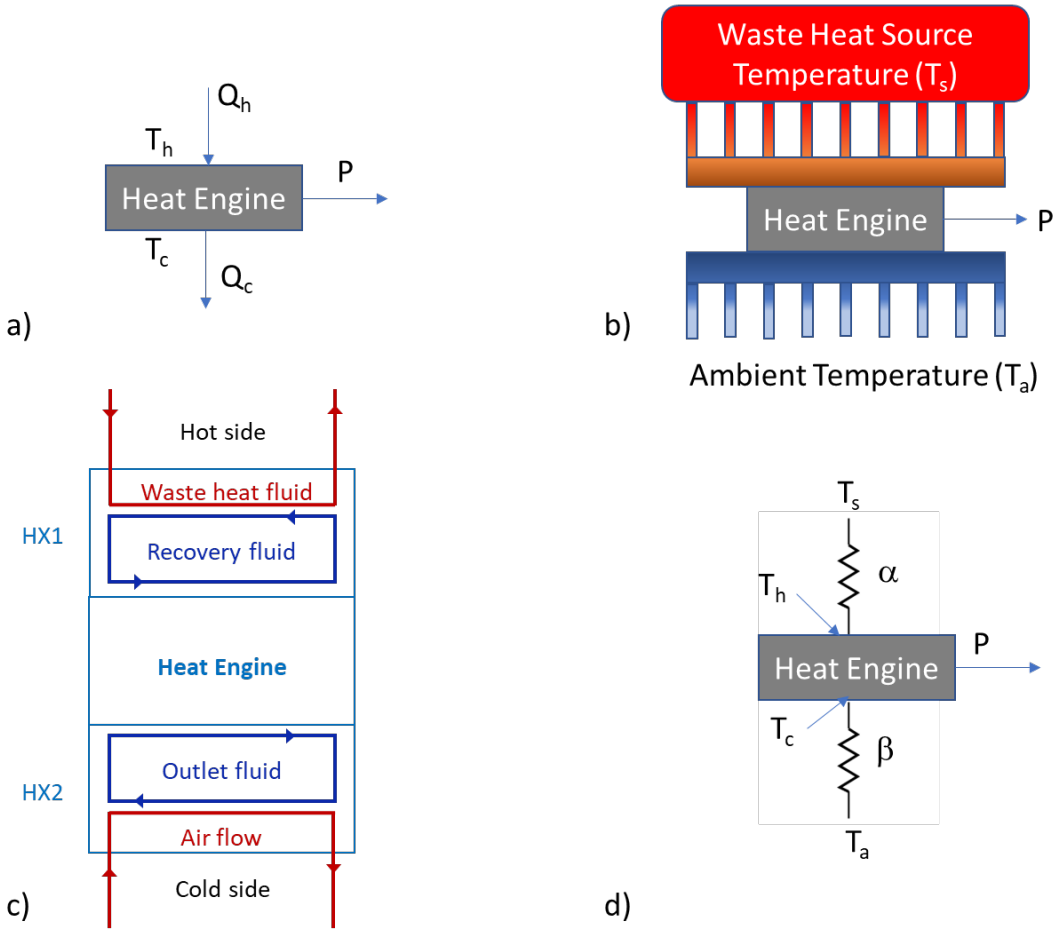

Figure 1: a) Typical lab-scale thermal setup (ideal) to evaluate performance of new WHC heat engines ensuring constant-temperature boundary conditions on the hot and cold

sides. T_h and T_c are the temperature of the engine on the hot side and cold side respectively; Q_h and Q_c are the heat input and heat rejection on the hot side and cold side respectively; p is the power output of the engine b) Schematic of real embodiment of WHC where hot-side and cold-side heat exchangers are needed c) Schematic representation of the thermal system. The hot side has a waste-heat fluid that transfers energy to a recovery fluid, and the cold side has water or an organic liquid as the hot fluid, and air as the final fluid to dissipate the heat to the ambient. d) Resistive network used to develop the endoreversible-thermodynamics-based TEA model. α and β are thermal conductances of the hot and cold side heat exchangers, respectively.

In this perspective we ask three simple questions to understand under what conditions WHC can be economically competitive with other zero carbon technologies, irrespective of the physical origin of the WHC system:

1) What is the required minimum temperature of the heat source?
2) What is the required minimum size (power output) of the WHC engine?
3) What is the minimum capacity factor i.e. what fraction of the time in a year is waste heat source available?

To answer these questions, we develop a TEA model for WHC based on the classic endoreversible [26–28] thermodynamic formulations developed by Curzon and Ahlborn, enabling the construction of a model that is independent of the specifics of the heat engine. In the endoreversible formulation, the heat engines are completely reversible (Carnot engines), and the irreversibility in the system is due to the heat exchangers. This provides the best-case scenario for the cost of the system. Finally, we include the irreversibility of the engine by modifying the endoreversible formulation and provide a cost target for novel heat engines as a function of the waste-heat temperature, power output, and internal irreversibility (expressed as relative Carnot efficiency) of the heat engine for WHC to be competitive with other zero-carbon technologies. **Our results indicate that: 1) regardless of the type or efficiency WHC heat engines are not economically viable below 100 °C (significant research has focused on this regime as seen from Table 1) and 2) Even above 100 °C, WHC is economical only for power outputs in the range of 100 kW to 1 MW with a capacity factor of 0.9.** Finally, we conclude this perspective by providing a

future outlook on the research needed in the field of WHC heat engines for it to be technically and techno-economically viable.

Techno-Economic Analysis (TEA) Model Development

Figure 1a presents a schematic of the test setup typically used in lab-scale experiments to evaluate the performance of a new heat engine. Maximum care is taken to avoid a temperature drop between the hot/cold source and the heat engine, enabling evaluation of the intrinsic conversion efficiency of the heat engine. Because the focus is not on techno-economic optimization, this setup is ideal for understanding device performance and relating it to material properties as well as understanding the intrinsic irreversibility of the heat engine. However, in any practical system, this setup will not work because the cost of getting the heat in and out of the system must also be considered. Figure 1b presents a schematic of a real system with a heat exchanger between the hot/cold side and the heat engine.

Because the cost of the fuel in a waste-heat system is zero, analogous to a PV or a geothermal system, the goal is to extract the maximum power output from the system to minimize the levelized cost of electricity (LCOE)[29] given the capital cost of the system. The cost/electric power output ($/W) can be written as

$$C_u = C_{hx} + C_{he} = \frac{(\alpha C_h(\alpha) + \beta C_c(\beta))}{P_{max}} + C_{he}, \quad (1)$$

where C_{hx} and C_{he} are the cost of the heat exchanger and heat engine ($/W), respectively; α and β are the thermal conductance (W_{th}/K) of the hot-side and cold-side heat exchanger, respectively; $C_h(\alpha)$ and $C_c(\beta)$ are the cost of the hot-side and cold-side heat exchanger per unit thermal conductance ($/W_{th}/K$), respectively; and P_{max} is the maximum electrical power output that can be extracted from the system. The subscript *th* denotes thermal. Typically[30], heat exchangers are priced based on their thermal conductance rating. Here, α and β represent thermal conductance values defined as $\alpha, \beta \equiv UA$, where U is the heat-transfer coefficient and A is the total area of the heat exchangers. U depends on the thermal properties of the heat exchanger, such as the thermal conductivity of the heat transfer fluid, the heat exchanger material, and the design of the heat exchanger[30]. The range of thermal conductance values depend on the industry and application. For example, in microelectronics cooling[31], where the thermal energy level is in the range of ~10 - 100 Watts the conductance ranges from 10 W_{th}/K – 100 W_{th}/K because the heat exchangers are very

small, requiring smaller areas and leading to lower thermal conductance. In large scale industrial applications[30] (applicable for WHC) where thermal energy transport is in the range of kWs to MWs, the heat exchangers are very large and the thermal conductance ranges from 10^3 W_{th}/K – 10^6 W_{th}/K. Note the cost of a heat exchanger per unit thermal conductance depends on the size (i.e., α and β) of the heat exchanger [30] because it decreases with increasing area of the heat exchanger due to economies of scale.

Internally reversible (endoreversible) heat engine: The highest electrical power output (P_{max}) theoretically possible for the system shown in Fig. 1b is for a Carnot Engine where the irreversibility in the system is only due to the heat exchangers. Curzon and Ahlborn [26] developed the endoreversible formulation for exactly this case as shown in Eq. SI1 in the supplementary information (SI). With known P_{max}, C_u in Eq. 1 can be optimized with respect to α and β to obtain the lowest possible cost (See SI for optimization details). If C_h and C_c are independent of α and β, respectively then it can be shown through this optimization that the minimum cost of power per Watt is given by

$$C_u = \frac{\left(\sqrt{C_h}+\sqrt{C_c}\right)^2}{\left(\sqrt{T_s}-\sqrt{T_a}\right)^2} + C_{he}. \quad (2)$$

where T_s is the waste-heat source temperature; and T_a is the ambient temperature. Eq. (2) clearly shows that the cost of power per Watt increases with decreasing waste-heat temperature and increasing cost of both the hot-side and cold-side heat exchanger. Although Eq. (2) is simple and provides insight into cost of power as a function of waste heat temperature and cost of heat exchanger, it is generally inaccurate for small systems because C_h and C_c have a strong dependence on α and β for $\alpha, \beta < \approx 10^5 \frac{\mathrm{W}}{K}$, as shown in Fig. SI4. For $\alpha, \beta > \approx 10^5 \frac{\mathrm{W}}{K}$, C_h and C_c are nearly constant, and Eq. (2) holds. Figure (SI2) in SI also shows physically what these values of α and β mean in terms of the power output from a heat engine.

Internally irreversible heat engine: In reality there will be internal entropy generation in a heat engine. The effect of the irreversibility of engines is typically reported from experiments or device models as the relative Carnot efficiency (ϕ) for the boundary conditions shown in Fig. 1a. ϕ is for the case of maximum power output as the goal is to maximize the power output for WHC as discussed above. For example ϕ of thermoelectrics is different for maximum power and maximum efficiency case (see SI). Table (1) shows range of relative Carnot efficiency for various heat engines. Howe [32] derived the power equation by considering both internal irreversibility and the

irreversibility due to the heat exchanger as shown in Eq. (SI2). For ϕ= 1, Howe's equation reduced to the endoreversible equation (SI1). We use Howe's equation to understand the impact of internal irreversibility on the cost of power output from WHC heat engines (See SI for optimization details).

Cost of heat exchangers : The cost of the heat exchanger depends on many factors including the material and type of heat exchanger and the heat-transfer fluid used in the heat exchanger. The selection of the material and type of heat exchanger along with the heat transfer fluid depend on the temperature of operation. The ESDU database [30,33] provides comprehensive cost data on the most common heat exchanger designs (shell-and-tube, double-pipe, welded, plate, plate-fin printed-circuit, and air-cooled heat exchanger) with thermal conductance ranging from 10^3 (W_{th}/K) to 10^6 (W_{th}/K). The ESDU database also provides a large variety of different heat transfer fluids for the hot and cold side (gases at low/medium/high pressure, water/steam, organic liquids, hydrocarbons, low/medium/high viscosity liquids), resulting in many different combinations of exchanger design and heat transfer fluids, each with different costs [$C_h(\alpha)$ and $C_c(\beta)$ in Eq. 1]. The selection of fluid depends on the temperature and compatibility with the heat exchanger material. Using data from the ESDU database, our analysis is based on a physical model of WHC with two fluids on the hot side and two fluids on the cold side (Fig. 1c). The calculations are conducted for two scenarios: 1) liquid is used as the recovery fluid on the hot side and 2) air is used as the recovery fluid for convenience because it can be used over a large temperature range and does not suffer from other complexities such as corrosion. For both scenarios, if T_c, as shown in Fig. 1d (see cost optimization section in SI for details), is below 100 °C, then water is used as the cold-side fluid; otherwise, organic liquid is used for T_c between 100 °C and 400 °C. Water is used for Tc < 100 °C as it is inexpensive, resulting in low $C_c(\beta)$. Finally, in both scenarios, the heat exchanger was selected based on the temperature range of operation and cost (the lowest-cost heat exchanger was selected for each temperature range). Table (2) provides a summary of the combinations of heat transfer fluid and heat exchanger depending on the temperature of the heat source.

For cost optimization, the cost functions $C_h(\alpha)$ and $C_c(\beta)$ were modeled using a power-law fitting curve ($C\ (\alpha) = a\alpha^b + c$) for the cost data from the ESDU database. The curve fits are presented in Fig. SI4. The error spread between the predicted and observed values for each combination of heat exchanger was computed using the root mean square relative error and showed a reasonable

fitting error with a maximum of 15%. The costs provided by the ESDU database were compiled in 1992. The costs were updated for 2020 (see SI). Table (2) lists the values of a, b, and c for the two scenarios described in the paper. We have assumed the ambient temperature to be 300 K. Since air is the final heat transfer fluid and the ambient temperature is fixed, the cold side heat exchanger and outlet fluid (Fig. 1c) are known, as opposed to the hot side heat exchanger where the temperature can vary significantly depending on the waste heat source. Therefore, cost minimization with respect to α was achieved numerically for fixed β (see SI). The optimal value of α, which gives the lowest value of C_u, is presented for scenario 1 in the SI (Table SI2). Finally, C_{hx} was calculated using Eq. 1.

	Waste-heat temperature (°C)	Waste-heat fluid – Recovery fluid	Hot-side heat exchanger type & curve-fit parameters (a,b,c)	Cold-side engine temperature, T_C (°C)	Cold-side outlet fluid	Cold-side heat exchanger type and curve-fit parameters (a,b,c)
Scenario 1	<100	Water – Water	(517.37, 0.82, 0.03) Plate heat exchanger	<100	Water	(18023, -0.90, 0.90) Air-cooled heat exchanger
	100 – 175	Organic liquid – Organic liquid	(348.61, -0.75 ,0.13) Plate heat exchanger	100 – 400*	Organic liquid	(13417, -0.85, 1.66) Air-cooled heat exchanger
	175 – 400	Organic liquid – Organic liquid	(1255.1, -0.74, 0.35) Double pipe			
	>400	Molten salt – Molten salt	(6166, -0.88, 1.89) Shell-and-tube			
Scenario 2	<100	Water - Air	(56401, -0.87, 1.53) Shell-and-tube	<100	Water	(18023, -0.90, 0.90) Air-cooled heat exchanger
	100 – 400	Organic liquid - Air	(59043, -0.87, 1.58) Shell-and-tube	100 – 400*	Organic liquid	(13417, -0.85, 1.66) Air-cooled heat exchanger
	>400	Molten Salt - Air	(60557, -0.87, 2.44) Shell-and-tube			

Table 2: Summary of heat exchanger and heat transfer fluid combinations for scenario 1 and scenario 2. *Cold side engine temperature (T_c) never exceeded 400 °C for the cases investigated in the paper.

Cost of heat engine: The Cost of novel heat engines is a big unknown. For rotary turbine-based heat engines the cost is known with a high level of confidence. For example the cost of an ORC turbine is 0.375/W [34] and a gas turbine which is ~$0.25/W [34]. Among non-rotary heat engines, thermoelectrics are probably the most mature; however, there is a great deal of uncertainty regarding its cost due to the lack of mass market and field data. Any reasonable estimate will put that cost to be much higher than $1/W[35]. Because the cost of the heat exchanger is known with a high level of confidence from published databases such as that of the ESDU and the cost of novel heat engines are relatively unknown, we derive the allowable cost of heat engines such that they meet the total capital cost target (see the results section).

Cost target for WHC: For WHC to become a serious and scalable contender, it must compete with other technologies such as solar PV, wind, and geothermal where both the cost of input energy and the carbon output is zero. All of these technologies have a similar levelized cost of electricity (LCOE) [36]. The LCOE depends on many factors including the overnight capital cost of energy conversion, the capacity factor, and operational/maintenance[34] costs. The TEA model developed in this perspective is for the overnight capital cost of energy conversion (engine and heat exchanger). A brief discussion of LCOE where cost of input energy is zero is provided in the SI. As shown in Eq. SI19, LCOE is directly proportional to the capital cost and inversely proportional to the capacity factor. It also depends on the lifetime of the technology which is related to the reliability. Longer lifetimes lead to lower LCOE. In addition, the discount rate, which accounts for the financing cost of the technology, also affects the LCOE; A lower discount rate lowers the LCOE. Therefore, for the same LCOE, a higher capital cost can be tolerated for higher capacity factors, longer lifetimes, and/or lower discount rates. For mature zero carbon technologies such as PV or geothermal power plants, the lifetime based on field data is in the range of 25 years[29] or longer, as they are highly reliable. Similarly, the typical discount rate is assumed to be ~6%[37]. The discount rate is typically higher for new/unproven technology. For similar lifetimes and discount

rates the allowable capital cost is proportional to the capacity factor for a desired LCOE. For example, solar PV only has a capacity factor of 30%, whereas geothermal power has a capacity factor of 90%[36]. Therefore, the allowable capital cost of energy conversion for solar PV (module cost) is much smaller than that for geothermal power (turbine and heat exchanger).

For novel WHCs, there is uncertainty regarding lifetime and discount rate due to lack of data. As a baseline in this perspective, we assume that WHCs have similar lifetimes and discount rates compared to mature zero carbon technologies. This is a highly optimistic assumption for non-ORC based WHCs because lifetime/reliability is a big unknown and, in reality, discount rates will be higher due to the perceived financial risk of a new technology. For the baseline we optimistically assume that the heat is available 90% of the year, i.e., it has a capacity factor of 90%. This allows for a much higher capital cost for WHC. Thus, the capital cost of WHC must be similar to that of geothermal electricity. In fact, geothermal power plants are very similar in nature to WHC even physically because the cost of heat is zero (as for WHC). The capital cost of power conversion in geothermal power plants is \$1.2/W [34] (ORC turbine and heat exchanger). Because most mature technologies have similar LCOE, the capital cost is set by the capacity factor when the discount rate and lifetime are equal. Thus, by optimistically assuming a capacity factor of 90%, we can take the capital cost of geothermal as the most optimistic target price-point in which WHC will have a LCOE competitive with current mature technologies. To be competitive then, we set the baseline cost target (C_u) to be \$1.2/W.

Figure (2) shows the cost target using Eq.SI19 for the cases where these optimistic assumptions are relaxed, assuming the LCOE remains the same as that of the baseline**.** Figure (2) shows that to maintain the same LCOE the capital cost has to be significantly lower for reduced capacity factor, reduced lifetime, and increased discount rate. Capital cost is directly proportional to the capacity factor for a given LCOE but is a more complicated function of the lifetime and discount rate. As shown in the SI, under the extreme case of zero discount rate the capital cost is directly proportional to the lifetime. For very long lifetimes, the capital cost is inversely proportional to the discount rate.

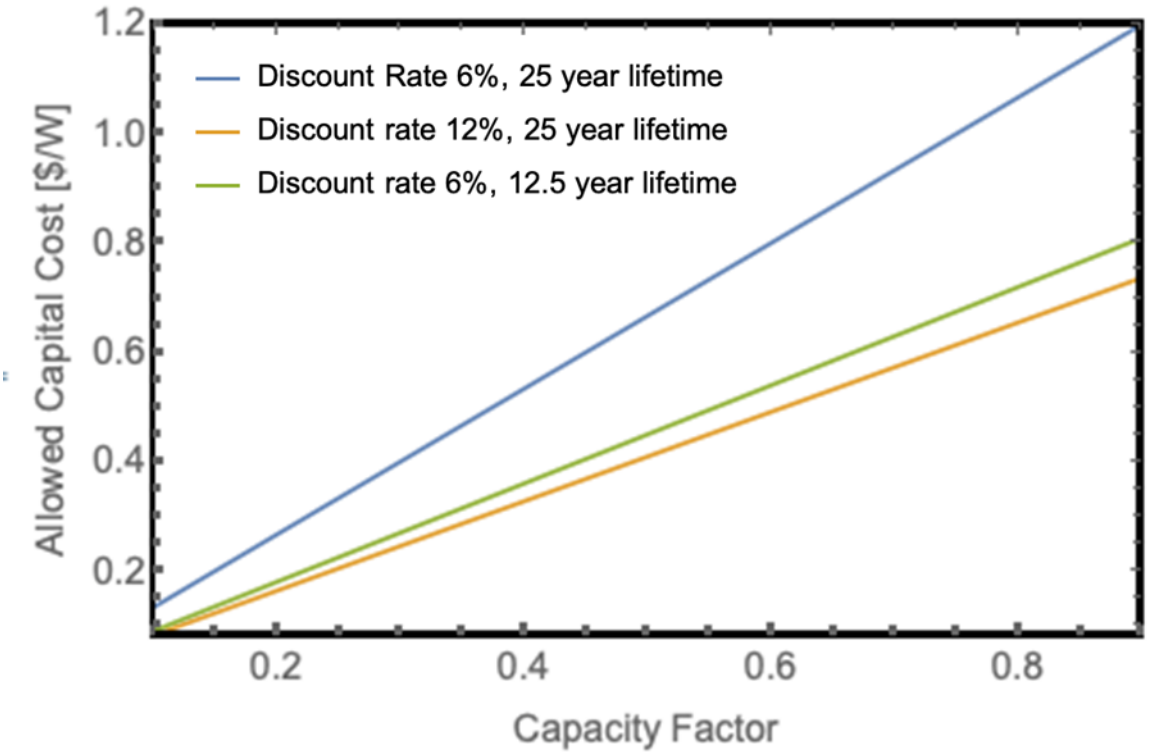

Figure 2: Allowed capital cost for constant LCOE as function of capacity factor for various lifetime of the WHC and discount rate.

Results

Endoreversible engine: In our calculations we assume that the ambient temperature is 300 °K. We plot the cost of heat exchanger per unit electrical power output, C_{hx}, in Figs. 3a and 3b first. We then use the known C_{hx} to derive the allowable cost of heat engine, C_{he}, (Figs. 3c and 3d) to meet the total capital cost target of \$1.2/W, i.e., $C_{he} = 1.2 - C_{hx}$. Fig. 2a shows that for a small cold side heat exchangers reflected in small value of cold side heat exchanger thermal conductance, β, even for this highly ideal case of a reversible heat engine, C_{hx} itself is much higher than the total target of \$1.2/W for temperatures below 300 °C (i.e., for these values of β and corresponding hot side heat exchanger thermal conductance,α,, WHC is not cost effective below 300 °C). Note for each β, optimal α is obtained by the cost optimization (see SI). Table SI1 in the SI lists α for various values of β. Even for 300 °C, the power required (size of the heat engine) to achieve a heat exchanger cost of \$1.2/W is ~40 kW (calculated using Eq. SI1); i.e., the size of the WHC engine must be in multiples of kWs.

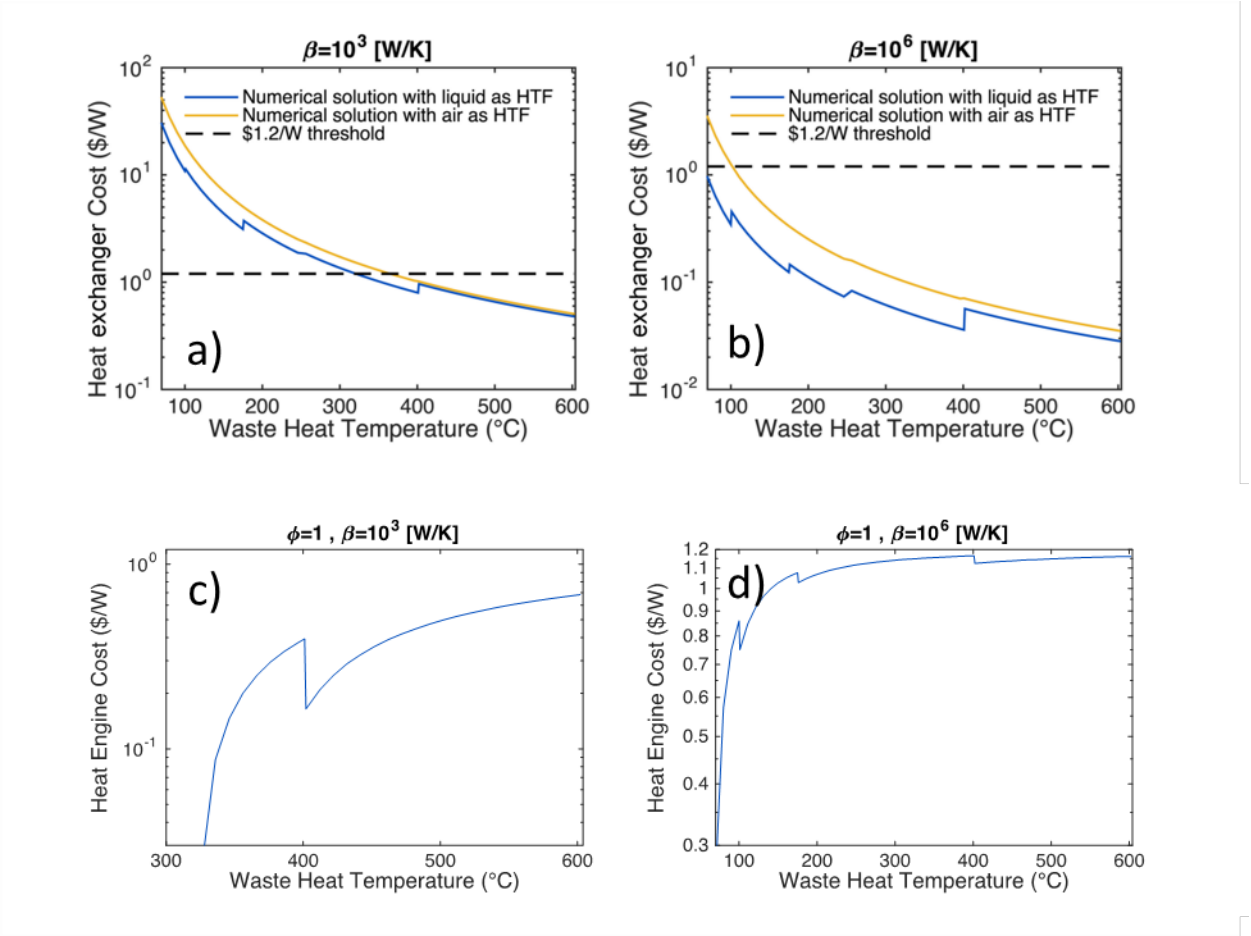

Figure 3: Cost of heat exchanger (C_{hx}) per unit electrical power output as a function of waste-heat source temperature and thermal conductance (β) of the cold-side heat exchanger for endoreversible engine (relative Carnot efficiency, ϕ =1). The results are shown for liquid and air as the recovery heat transfer fluid (see text and Table 1 for details). The kinks in the graph correspond to the sudden change of the cost of the heat echanger based on the fluid change/heat exchanger-type change depending on the temperature (see text for details). The dashed horizontal lines correspond to a capital cost (heat exchanger + heat engine) target of $1.2/W which assumes a capacity factor of 0.9. Figs. c and d show the required heat engine cost target (C_{he}) to maintain a total system cost of $1.2/W based on Eq. 1, i.e., $C_{he} = 1.2 - C_{hx}$.

For larger heat exchangers with $\beta = 10^6$ (W/K), it is possible for C_{hx} to be below $1.2/W for T ~ 50 °C; however, the size of the heat engine required is ~400 kW. Figures 3a and 3b also show that for the air-recovery fluid, C_{hx} is higher than for the liquid-based recovery fluid on the hot side

because of the low heat-transfer coefficient, which requires a larger surface area of the heat exchanger compared with that when using liquids.

Figures 3b and 3c show that the required heat engine cost, C_{he} = 1.2 - C_{hx}, to meet a cost target of \$1.2/W is very small at lower temperatures, particularly for low values of β. Because the endoreversible formulation is for an internally reversible engine, the results presented in Fig. 3 are a very optimistic scenario and provide the highest possible C_{he} to meet the cost target. In reality, internal irreversibility will reduce C_{he}. Note that the singularities in Fig. 3 are because of the change in the cost of the heat exchanger and fluid combination as a function of temperature. Higher temperature heat exchanger and fluid are more expensive than lower temperature heat exchanger and fluid. For example, above 100 ºC the fluid changes from water to organic liquid. This suddenly increases the cost of the heat exchanger at 100 ºC. However, the cost starts to go down as a function of temperature again. This behavior can be explained qualitatively using simplified Eq. 2 for the case where the cost of the heat exchanger per unit thermal conductance is independent of the thermal conductance. Since C_{he} = 1.2 - C_{hx}, this singularity at various temperatures shows up in the cost of the heat engines also. Table 2 shows that there are 3 temperatures at which cost changes (100 ºC, 175 ºC and 400 ºC). It can be seen from Fig. 3 that the singularities also appear exactly at these temperatures. The same behavior can be seen for the case of Irreversible engine as discussed below.

Irreversible engine: For irreversible engines the relative Carnot efficiency, ϕ, is a very important parameter and it depends on the type of engine. Table 1 shows the range of ϕ for various types of engines. Analogous to Fig. 3, Fig. 4 shows the cost of the heat exchanger, C_{hx}, and the allowable cost of the heat engine, C_{he} = 1.2 - C_{hx} for different ϕ. ϕ strongly affects C_{hx} and the allowable C_{he}. Optimal values of the hot side thermal conductance, α for the hot-side temperature and cold side thermal conductance, β are given in Table SI1. For $\beta = 10^3$ *W/K,* even for ϕ as high as 0.6, i.e., for engines working at 60% of Carnot efficiency, C_{hx} itself is much higher than the target of \$1.2/W. Figure 3c shows that for $\beta = 10^3$ *W/K*, there is no solution for C_{he} for ϕ <0.6 for reasonable waste-heat temperatures. Even for $\beta = 10^6$ *W/K*, C_{hx} is higher than the target below ~100 °C even for ϕ = 0.6. Figure 4 show that ϕ strongly affects the cost of the heat exchanger. Since for ORC, ϕ is large as compared to other novel heat engines the cost of the heat exchanger is very low. Therefore, geothermal plants based on ORC can operate for temperatures as low as 100 ºC.

Figure 5 shows C_{hx} as a function of the power output of the engine (see Eq. SI2). It shows that C_{hx} is a strong function of the power output and decreases significantly with increasing size of the engine. The curve of C_{hx} as a function of power output is smooth unlike that as a function of temperature (Fig. 4) because the temperature of the heat source is fixed for cost calculations as a function of power output, which fixes the type of heat exchanger and heat transfer fluid. Figure 5 also shows that the C_{hx} asymptotes as a function of size (power output) of the engine because cost of heat exchanger asymptotes as function of size of heat exchanger as shown in Fig. SI4. This type of asymptotic behavior has been reported for ORCs based on field data[24].

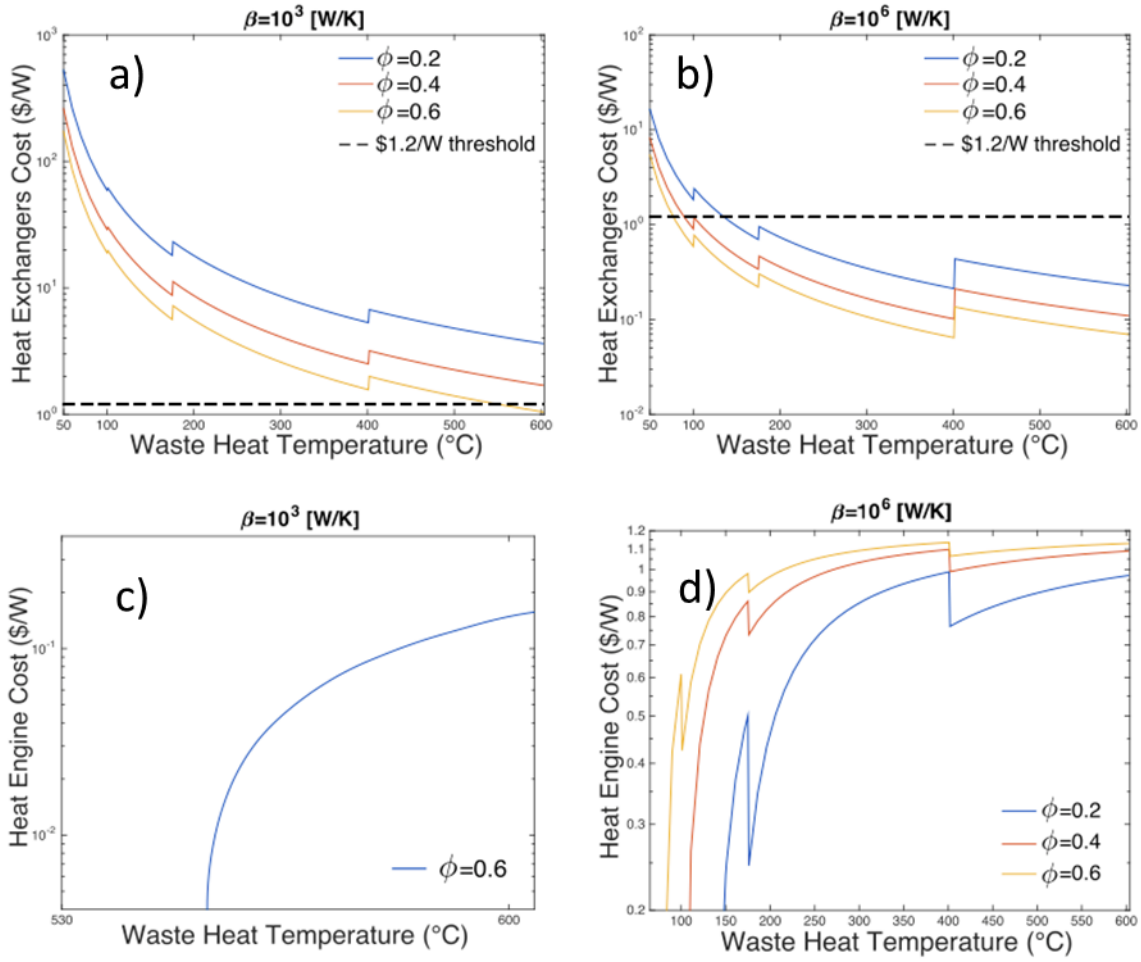

Figure 4: Cost of heat exchanger, C_{hx}, (a,b) and allowable cost of heat engine, C_{he}, (c,d) as a function of temperature, relative Carnot efficiency (ϕ) and thermal conductance (β) of the cold-side heat exchanger. The dashed horizontal lines correspond to a capital cost (heat exchanger + heat engine) target of $1.2/W which assumes a capacity factor of 0.9.

The kinks in the plot at various temperatures are due to changes in the heat exchanger /fluid combination on the hot side and cold side depending on the temperature based on the optimization algorithm (see SI and Table 1).

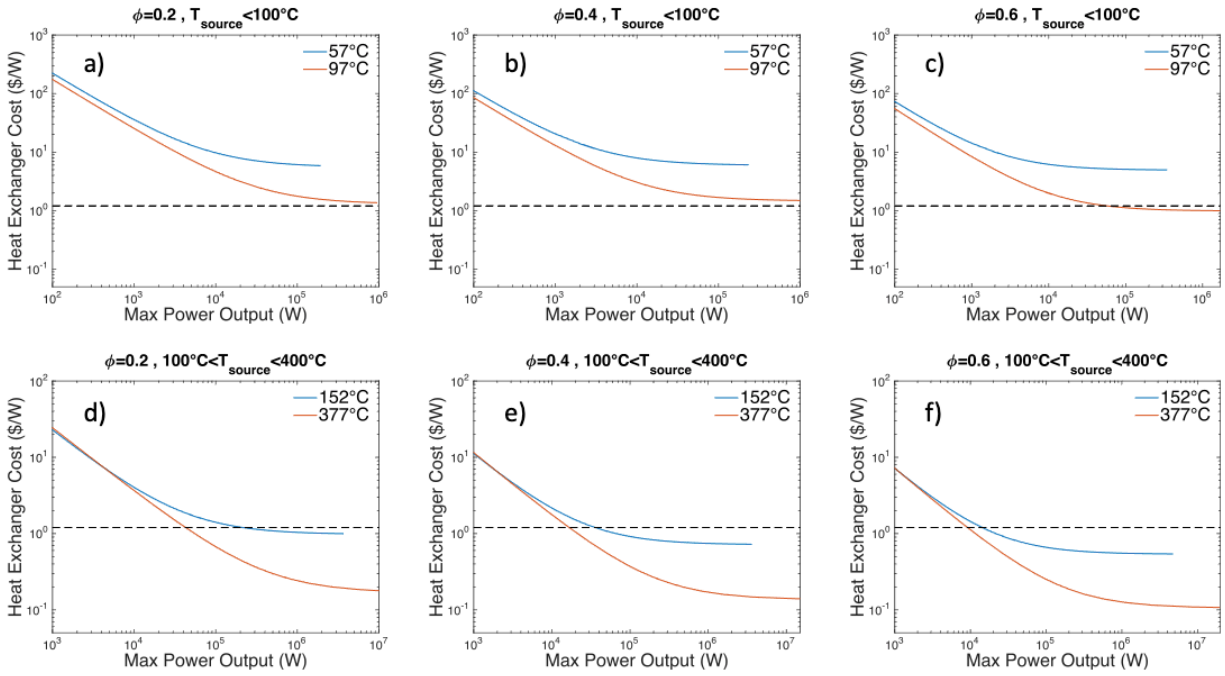

Figure 5: Cost of heat exchanger per unit electrical power output as a function of power for different values of relative Carnot efficiency (ϕ) and waste heat temperature (T_{source}). The dashed horizontal lines correspond to a capital cost (heat exchanger + heat engine) target of $1.2/W which assumes a capacity factor of 0.9. For T_{source} less than 100 °C, the cost of the heat exchanger itself is much higher than the target value for most values of power.

Figure 6 shows the allowable cost of the heat engine, C_{he}, as a function of power output. It shows that a larger heat engine can be more expensive than a smaller one because the cost of the heat exchanger is much smaller for a larger heat engine. Figures 4 and 5 show that WHC is not a

financially viable technology for temperatures < 100 °C and power output less than 100 kW even for $\phi = 0.6$.

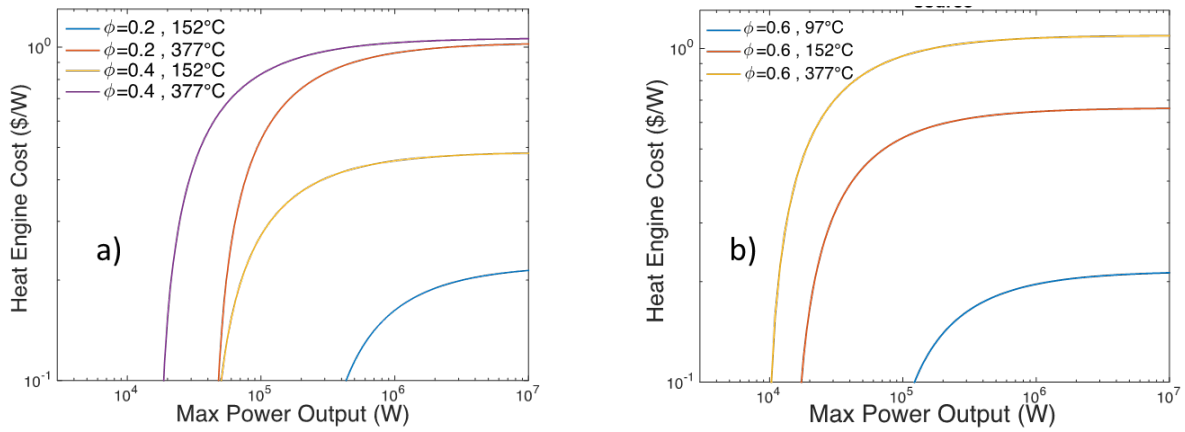

Figure 6: Allowable cost of heat engine. C_{he}, as a function of power output for different values of relative Carnot efficiency (ϕ) and waste heat temperature (T_{source}).

Discussion and Future Outlook

Minimum viable temperature and power output: Assuming that the best-case scenario for the cost of a heat engine is that it approaches that of large gas turbines (more than 100 years of innovation has gone into these turbines), which is ~$0.25/W[34], the allowed cost of the heat exchanger is then $0.95/W for a capacity factor of 0.9. Note even after 50 years of innovation the cost of ORC turbine is $0.375/W [34]. Among the non-rotary heat engines, thermoelectrics are probably the most mature option. The current cost of the thermoelectrics is expected to be significantly higher than $1/W[35]. Therefore, assuming the heat engine cost of $0.25/W is a highly optimistic scenario (in reality the number will be higher), Fig. 5d (blue curve) shows that WHC is not a viable technology for $\phi < 0.2$, $T_s < 152$ °C, and power output less than 1 MW if the cost of the heat exchanger remains the same as the historical numbers used in this perspective. **Various non-rotary heat engines typically report $\phi < 0.2$ (Table 1) so the cost of the heat exchanger alone would exceed the economic threshold, $1.2/W, for almost all low temperature waste heat energy conversion applications even for such a high capacity factor and low heat engine**

cost. Even for ϕ as high as 0.4, Fig. 5d shows that power output has to be greater than 100 kW+ for T_s > 152 ºC. In addition, because the capital cost requirement is lower than the baseline assumption cost of \$1.2/W for lower capacity factors (Fig. 2), the minimum viable temperature will increase to match the lower capital cost required for WHC with lower capacity factors. For example, for a capital cost of \$0.6/W which is the allowable cost for a capacity factor of 0.45 with a discount rate of 6% and lifetime of 25 years (Fig. 2) and with a heat engine cost of ~\$0.25/W, the allowable heat exchanger cost is \$0.35/W, which will increase the minimum viable temperature (Fig. 4b). Figure (7) shows the minimum viable temperature as a function of capacity factor assuming a 25-year lifetime and a discount rate of 6% (See SI for details). We have assumed a large heat exchanger ($\beta = 10^6$ W_{th}/K) as it gives the lowest cost as shown in Fig. 4. The minimum size of the heat engine for various conditions shown in Fig. (7) still varies between 100 kW – 1 MW. For higher discount rates or lower lifetimes, the minimum viable temperature will increase as the allowed capital cost will be lower (Fig. 2) and vice-versa.

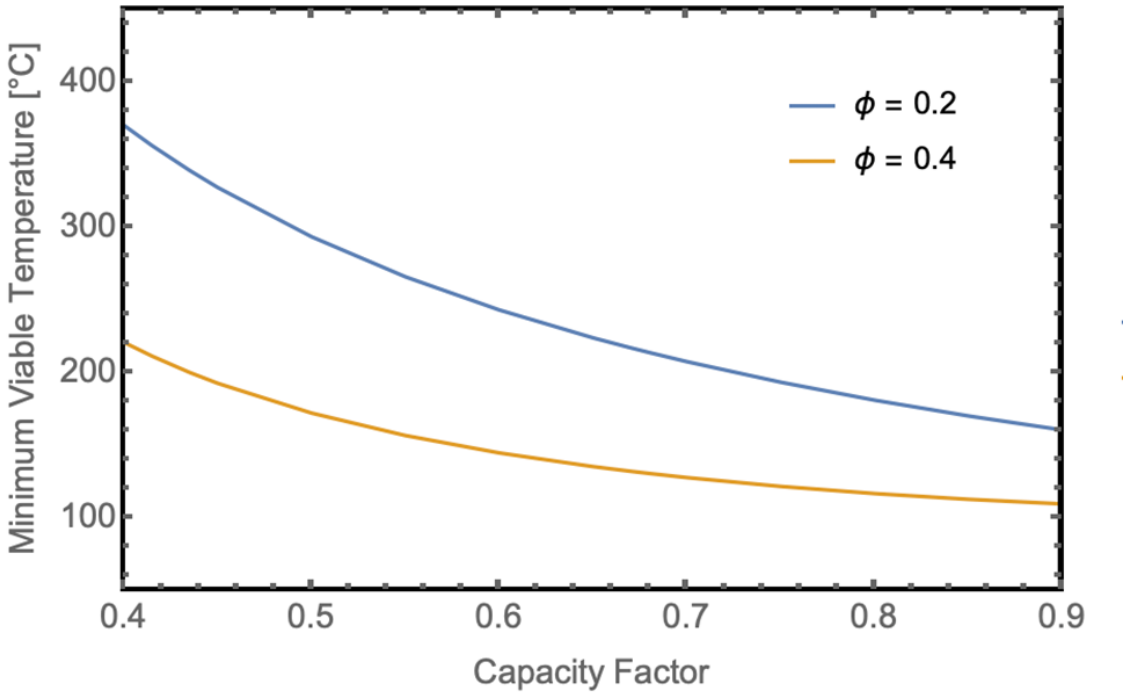

Figure 7: Minimum viable temperature as a function of capacity factor and different values of relative Carnot efficiency (ϕ) of the heat engine assuming a lifetime of 25 years and a discount rate of 6%**.** Note that for higher discount rate or lower lifetime the minimum viable temperature will increase as the allowed capital cost will be lower (Fig. 2). This

curve was generated assuming that the cost of the heat engine (C_{he}) is \$0.25/W which is the same as gas turbines (this is a highly optimistic assumption, see manuscript for details). For higher values of heat engine cost the curve will shift upwards and increase the minimum viable temperature. The minimum size of the heat engine for various conditions shown still varies between 100 kW – 1 MW.

Availability of high capacity factor and/or high temperature waste heat sources*:* As discussed one of the major factors that decides the economic viability of WHC is the capacity factor. WHC can be potentially economical at lower temperatures when coupled with high capacity factor sources. For lower capacity factor sources, a higher temperature waste-heat source is needed (Fig.7). Forman et al. [3] have provided a detailed description of temperature at which waste heat is available in the various sectors (Fig. SI1). In the following we discuss the viability of WHC for those sectors based on the data by Forman et al. [3].

1) Electricity: The largest amount of waste heat is available from this sector and typically the capacity factor of base load power plants (Coal, Nuclear and Natural gas combined cycle) is very high; however most of the waste heat available is at T < 100 ^{o}C because this the heat rejected by the steam condenser. There is some waste heat available at temperatures above 100^{o}C (Fig. SI1) due to waste heat in the flue gases, but the temperature is typically less than 120 ^{o}C. Therefore, it is highly unlikely that WHC is going to be economical in the electricity sector.
2) Industrial: This sector has waste heat available in the range of 100 – 300 ^{o}C and above 300 ^{o}C. There is a significant number of industries where the temperature is greater than 150 ^{o}C and the waste heat available is the range of MWs. The capacity factor of factories is typically very high (~1). In addition, the industrial sector is one of the hardest sectors to decarbonize[38]. Therefore, the industrial sector is one of the most promising sectors for the application of WHC. It's not surprising that most of the demonstration projects for WHC are in the industrial sector[39].
3) Residential: There is a significant amount of waste heat available above 100 ^{o}C in the residential sector due to heating furnaces and natural gas-based water heaters, but most of

that waste heat is at temperatures less than 150 °C. The yearly capacity factor of the heating furnaces is low because they are only operational during the winter months. Although water heaters are operational all year round, the capacity factor is not very high. Therefore, the low-capacity factor and lower temperatures available in the residential sector are discouraging for WHC.

4) Commercial: The commercial sector sees temperatures above 300 °C primarily because of diesel generators used to provide electricity. This is very prevalent in the developing and underdeveloped economies. Although the capacity factor is not very high, the high temperature waste heat can be economical even with lower capacity factor (Fig. 7).
5) Transportation: Like commercial, the transportation sector has an abundance of waste heat available above 300 °C resulting from the exhaust of flue gases from engines. However, the capacity factor in the transportation sector varies dramatically. For example, passenger cars in the US are driven for ~300 hours[40] every year which means the capacity factor is ~3%, whereas long haul transport, such as ships and trains, have a very high capacity factor. Similarly, aircrafts and long-haul trucks also have relatively high capacity factors. The waste heat available in these sectors is in the range of hundreds of kWs to a few MWs. These long-haul sectors within transportation are also very hard to decarbonize[41]. Therefore, combined with high temperature and an abundance of waste heat, the transportation sector can use heat engines that are more cost competitive. Moreover, relatively large capacity factors for these long-haul sectors of transportation make them promising candidates for WHC. For transportation, the cost target should be compared with savings in fuel cost such as diesel. More detailed analysis based on the framework proposed in this paper can be undertaken for the transportation sector.

Typically, waste heat literature only documents the amount of waste heat available along with the temperature of the waste heat source. As discussed in this perspective, the capacity factor of the waste heat should also be documented to evaluate the commercial viability of utilizing and converting that waste heat to electricity.

Advancement in heat engines: Based on this analysis the focus should be on the development of medium to high temperature heat engines. There have been recent advances on this front for both thermoelectrics[42,43] and other types of engines such as high temperature electrochemical heat

engines[21] and thermophotovoltaics[44]. As shown in Table 1, the relative Carnot efficiency of most non-rotary engines is below 0.2. For the high temperature electrochemical heat engine, the relative Carnot efficiency of 0.3 is based on system level simulation and experimental demonstration is still needed. As shown in Fig. 7, the minimum viable temperature reduces significantly for higher relative Carnot efficiency which can open up more opportunities as discussed above for WHC. Another potential area of research, which has received little to no attention, is on the reliability of novel waste heat engines. Since the LCOS is a strong function of lifetime of the technology, it is important to understand the long-term performance of the heat engine, particularly at higher temperatures. New protocols should be developed for accelerated lifetime testing of novel heat engines to understand their long-term behavior and commercial viability.

Advancement in heat exchangers: The bleak prospective for heat engines as waste heat converters for lower temperature assumes the cost of heat exchangers follows the historical heat exchanger price trend. Major innovations[45,46] in heat exchanger design are being made with new manufacturing techniques that could provide disruptive cost advantages. If the cost of heat exchangers can be significantly decreased, there is far more opportunity for heat engines in the waste heat conversion space. For example, the advent of additive manufacturing and topology optimization may lead to a shift in the cost of heat exchangers as a function of size. This could potentially bend the cost curves and reduce the minimum viable temperature for WHC; however, it is highly unlikely that WHC below 100 °C will be economically viable even in these best-case scenarios.

Energy Storage, Dispathability and time value of Electricity: Finally, other zero carbon technologies such as PV or wind are intermittent. Large scale deployment of these intermittent technologies will require significant breakthroughs in energy storage[47]. On the other hand, geothermal electricity is available all day and is dispatchable (i.e. its power can be switched on and off depending on the demand on the electricity grid). For WHC with a high-capacity factor (e.g. industrial), it's possible to make it dispatchable; however unlike geothermal the waste heat will get wasted unless its stored in a thermal storage. To get electricity back from thermal storage the temperature must be high enough for higher thermodynamic conversion efficiency and the cost of the storage must be very low so that there is not much impact on LCOE. This needs further

investigation. For lower capacity factor systems, it is possible to increase the capacity factor of the WHC by storing the energy in thermal storage and using WHC directly from the waste source and from the thermal storage when the waste heat source is not available with lower average power. This is analogous to a concentrated solar plant (CSP), where thermal storage enables higher capacity factor for the steam turbine[48]. However, analogous to CSP, the cost of thermal storage has to be low and temperature of the waste heat source has to be high. These scenarios can be investigated relatively easily using the techno-economic framework for WHC proposed in this perceptive.

The price and value of electricity can also be dependent on the time of the day and there is growing use of time-of-use rate plans for electricity price[49]. Through the TEA model proposed in this perspective more studies should be undertaken to understand if higher capital cost of WHC can be accommodated even for lower capacity factors if the price of electricity varies significantly during the day.

Conclusion

In this perspective we have introduced a TEA model for waste heat conversion based on the endoreversible thermodynamics formulation which makes the TEA independent of the specifics of the heat engine technology. The TEA is mainly dependent on technological parameters such as temperature of the waste heat source, cost of heat exchangers, and relative Carnot efficiency of the heat engine. Through this TEA model we have calculated the minimum viable temperature for cost effective waste heat conversion. However, further detailed studies for various energy sectors should be conducted to understand the commercial viability of waste heat conversion. Tabulation of capacity factors for various waste heat sources should also be documented in the future.

Acknowledgments: The authors acknowledge the support of from California Energy Commission EPC-16-042. RP would also like to acknowledge Dr. Dane Boysen for valuable discussions and for motivating him to explore this topic.

Author Contributions: RP came up with the original idea of developing the TEA model and supervised the work. PSP conducted the initial literature search and analytical calculation assuming that the cost was independent of the size of the heat exchanger. CG developed the

solution for the size-dependent cost. DL performed the calculation for thermoelectrics. DL and CG worked on the development of the numerical methods. RP wrote the paper. RP supervised the work.

References

1. Landry, B.A. (1953). Utilization of waste heat. Science (80-.). *117*, 3.
2. Wakao, N., and Nojo, K. (1978). Nitric acid cycle process for extracting thermal energy from low-level heat sources. Nature *273*, 25–27.
3. Forman, C., Muritala, I.K., Pardemann, R., and Meyer, B. (2016). Estimating the global waste heat potential. Renew. Sustain. Energy Rev. *57*, 1568–1579.
4. Boukai, A.I., Bunimovich, Y., Tahir-Kheli, J., Yu, J.K., Goddard, W.A., and Heath, J.R. (2008). Silicon nanowires as efficient thermoelectric materials. Nature *451*, 168–171.
5. Hochbaum, A.I., Chen, R., Delgado, R.D., Liang, W., Garnett, E.C., Najarian, M., Majumdar, A., and Yang, P. (2008). Enhanced thermoelectric performance of rough silicon nanowires. Nature *451*, 163–167.
6. Waske, A., Dzekan, D., Sellschopp, K., Berger, D., Stork, A., Nielsch, K., and Fähler, S. (2019). Energy harvesting near room temperature using a thermomagnetic generator with a pretzel-like magnetic flux topology. Nat. Energy *4*, 68–74.
7. Yu, B., Duan, J., Cong, H., Xie, W., Liu, R., Zhuang, X., Wang, H., Qi, B., Xu, M., Wang, Z.L., et al. (2020). Thermosensitive crystallization-boosted liquid thermocells for low-grade heat harvesting. Science (80-.). *370*, 342–346.
8. Straub, A.P., Yip, N.Y., Lin, S., Lee, J., and Elimelech, M. (2016). Harvesting low-grade heat energy using thermo-osmotic vapour transport through nanoporous membranes. Nat. Energy *1*, 1–6.
9. Wang, X., Huang, Y.T., Liu, C., Mu, K., Li, K.H., Wang, S., Yang, Y., Wang, L., Su, C.H., and Feng, S.P. (2019). Direct thermal charging cell for converting low-grade heat to electricity. Nat. Commun. *10*, 1–8.
10. Li, T., Zhang, X., Lacey, S.D., Mi, R., Zhao, X., Jiang, F., Song, J., Liu, Z., Chen, G., Dai,

J., et al. (2019). Cellulose ionic conductors with high differential thermal voltage for low-grade heat harvesting. Nat. Mater. *18*, 608–613.

11. Lee, S.W., Yang, Y., Lee, H.W., Ghasemi, H., Kraemer, D., Chen, G., and Cui, Y. (2014). An electrochemical system for efficiently harvesting low-grade heat energy. Nat. Commun. *5*, 1–6.

12. Venkatasubramanian, R., Siivola, E., Colpitts, T., and O'Quinn, B. (2001). Thin-film thermoelectric devices with high room-temperature figures of merit. Nature *413*, 597–602.

13. Venkatasubramanian, R. (2019). Power from nano-engineered wood. Nat. Mater. *18*, 536–537.

14. Shaulsky, E., Boo, C., Lin, S., and Elimelech, M. (2015). Membrane-based osmotic heat engine with organic solvent for enhanced power generation from low-grade heat. Environ. Sci. Technol. *49*, 5820–5827.

15. Bell, L.E. (2008). Cooling, heating, generating power, and recovering waste heat with thermoelectric systems. Science (80-.). *321*, 1457–1461.

16. Im, H., Kim, T., Song, H., Choi, J., Park, J.S., Ovalle-Robles, R., Yang, H.D., Kihm, K.D., Baughman, R.H., Lee, H.H., et al. (2016). High-efficiency electrochemical thermal energy harvester using carbon nanotube aerogel sheet electrodes. Nat. Commun. 2016 71 *7*, 1–9.

17. Duan, J., Feng, G., Yu, B., Li, J., Chen, M., Yang, P., Feng, J., Liu, K., and Zhou, J. (2018). Aqueous thermogalvanic cells with a high Seebeck coefficient for low-grade heat harvest. Nat. Commun. *9*, 1–8.

18. Pandya, S., Wilbur, J., Kim, J., Gao, R., Dasgupta, A., Dames, C., and Martin, L.W. (2018). Pyroelectric energy conversion with large energy and power density in relaxor ferroelectric thin films. Nat. Mater. *17*, 432–438.

19. Fitriani, Ovik, R., Long, B.D., Barma, M.C., Riaz, M., Sabri, M.F.M., Said, S.M., and Saidur, R. (2016). A review on nanostructures of high-temperature thermoelectric materials for waste heat recovery. Renew. Sustain. Energy Rev. *64*, 635–659.

20. Thakre, A., Kumar, A., Song, H.C., Jeong, D.Y., and Ryu, J. (2019). Pyroelectric energy conversion and its applications—flexible energy harvesters and sensors. Sensors

(Switzerland) *19*, 2170.

21. Poletayev, A.D., McKay, I.S., Chueh, W.C., and Majumdar, A. (2018). Continuous electrochemical heat engines. Energy Environ. Sci. *11*, 2964–2971.

22. Feng, H., Chen, W., Chen, L., and Tang, W. (2020). Power and efficiency optimizations of an irreversible regenerative organic Rankine cycle. Energy Convers. Manag. *220*, 113079.

23. Wang, J., Yan, Z., Wang, M., Li, M., and Dai, Y. (2013). Multi-objective optimization of an organic Rankine cycle (ORC) for low grade waste heat recovery using evolutionary algorithm. Energy Convers. Manag. *71*, 146–158.

24. Quoilin, S., Broek, M. Van Den, Declaye, S., Dewallef, P., and Lemort, V. (2013). Techno-economic survey of organic rankine cycle (ORC) systems. Renew. Sustain. Energy Rev. *22*, 168–186.

25. Yee, S.K., Leblanc, S., Goodson, K.E., and Dames, C. (2013). $ per W metrics for thermoelectric power generation: Beyond ZT. Energy Environ. Sci. *6*, 2561–2571.

26. Curzon, F.L., and Ahlborn, B. (1975). Efficiency of a Carnot engine at maximum power output. Am. J. Phys. *43*, 22–24.

27. Van Den Broeck, C. (2005). Thermodynamic efficiency at maximum power. Phys. Rev. Lett. *95*, 190602.

28. De Vos, A. (1992). Endoreversible Thermodynamics of Solar Energy Conversion (Oxford Science).

29. Branker, K., Pathak, M.J.M., and Pearce, J.M. (2011). A review of solar photovoltaic levelized cost of electricity. Renew. Sustain. Energy Rev. *15*, 4470–4482.

30. Hewitt, G.F., and Pugh, S.J. (2007). Approximate design and costing methods for heat exchangers. Heat Transf. Eng. *28*, 76–86.

31. Lee, S. (1995). Optimum Design and Selection of Heat Sinks. IEEE Trans. Components Packag. Manuf. Technol. Part A *18*, 812–817.

32. Howe, J.P. (1982). The maximum power, heat demand and efficiency of a heat engine operating in steady state at less than Carnot efficiency. Energy *7*, 401–402.

33. Selection and Costing of Heat Exchangers ESDU 92013 (1994).

34. U.S Energy Information Administration(EIA) (2020). Capital Cost and Performance Characteristic Estimates for Utility Scale Electric Power Generating Technologies.

35. Leblanc, S., Yee, S.K., Scullin, M.L., Dames, C., and Goodson, K.E. (2014). Material and manufacturing cost considerations for thermoelectrics. Renew. Sustain. Energy Rev. *32*, 313–327.

36. U.S. Energy Information Administration (2021). Levelized Costs of New Generation Resources in the Annual Energy Outlook 2021.

37. Analysis, I. (2002). The Electricity Market Module of the National Energy Modeling System Model Documentation Report. Energy *068*.

38. Thiel, G.P., and Stark, A.K. (2021). To decarbonize industry, we must decarbonize heat. Joule *5*, 531–550.

39. Elson, A., Tidball, R., and Hampson, A. (2015). Waste Heat to Power Market Assessment. Oakridge National Lab, Report no. ORNL/TM-2014/620

40. Johnson, T. (2016). Americans Spend an Average of 17,600 Minutes Driving Each Year. AAA, 1. https://newsroom.aaa.com/2016/09/americans-spend-average-17600-minutes-driving-year/.

41. Majumdar, A., Deutch, J.M., Prasher, R.S., and Griffin, T.P. (2021). A framework for a hydrogen economy. Joule *5*, 1905–1908.

42. Jiang, B., Yu, Y., Cui, J., Liu, X., Xie, L., Liao, J., Zhang, Q., Huang, Y., Ning, S., Jia, B., et al. (2021). High-entropy-stabilized chalcogenides with high thermoelectric performance. Science (80-.). *371*, 830–834.

43. Zhou, C., Lee, Y.K., Yu, Y., Byun, S., Luo, Z.Z., Lee, H., Ge, B., Lee, Y.L., Chen, X., Lee, J.Y., et al. (2021). Polycrystalline SnSe with a thermoelectric figure of merit greater than the single crystal. Nat. Mater., 1–7.

44. Burger, T., Sempere, C., Roy-Layinde, B., and Lenert, A. (2020). Present Efficiencies and Future Opportunities in Thermophotovoltaics. Joule *4*, 1660–1680.

45. Stark, A.K., and Klausner, J.F. (2017). An R&D Strategy to Decouple Energy from Water.

Joule *1*, 416–420.

46. Moon, H., McGregor, D.J., Miljkovic, N., and King, W.P. (2021). Ultra-power-dense heat exchanger development through genetic algorithm design and additive manufacturing. Joule *0*.

47. Albertus, P., Manser, J.S., and Litzelman, S. (2020). Long-Duration Electricity Storage Applications, Economics, and Technologies. Joule *4*, 21–32.

48. SunShot Vision Study | Department of Energy https://www.energy.gov/eere/solar/sunshot-vision-study.

49. Zurfi, A., Albayati, G., and Zhang, J. (2017). Economic feasibility of residential behind-the-meter battery energy storage under energy time of-use and demand charge rates. In 2017 6th International Conference on Renewable Energy Research and Applications, ICRERA 2017 (Institute of Electrical and Electronics Engineers Inc.), pp. 842–849.

Figure Legend:

Figure 1: Modeling of Heat Engines

Typical lab-scale thermal setup (ideal) to evaluate performance of new WHC heat engines ensuring constant-temperature boundary conditions on the hot and cold sides. T_h and T_c are the temperature of the engine on the hot side and cold side respectively; Q_h and Q_c are the heat input and heat rejection on the hot side and cold side respectively; p is the power output of the engine b) Schematic of real embodiment of WHC where hot-side and cold-side heat exchangers are needed c) Schematic representation of the thermal system. The hot side has a waste-heat fluid that transfers energy to a recovery fluid, and the cold side has water or an organic liquid as the hot fluid, and air as the final fluid to dissipate the heat to the ambient. d) Resistive network used to develop the endoreversible-thermodynamics-based TEA model. □ and □ are thermal conductances of the hot and cold side heat exchangers, respectively.

Figure 2: Allowed capital cost for constant LCOE as function of capacity factor for various lifetime of the WHC and discount rate.

Figure 3: Cost of heat exchanger (C_{hx}) per unit electrical power output as a function of waste-heat source temperature and thermal conductance (β) of the cold-side heat exchanger for endoreversible engine (relative Carnot efficiency, ϕ =1). The results are shown for liquid and air as the recovery heat transfer fluid (see text and Table 1 for details). The kinks in the graph correspond to the sudden change of the cost of the heat echanger based on the fluid change/heat exchanger-type change depending on the temperature (see text for details). The dashed horizontal lines correspond to a capital cost (heat exchanger + heat engine) target of $1.2/W which assumes a capacity factor of 0.9. Figs. c and d show the required heat engine cost target (C_{he}) to maintain a total system cost of $1.2/W based on Eq. 1, i.e., $C_{he} = 1.2 - C_{hx}$.

Figure 4: Cost of heat exchanger, C_{hx}, (a,b) and allowable cost of heat engine, C_{he}, (c,d) as a function of temperature, relative Carnot efficiency (ϕ) and thermal conductance (β) of the cold-side heat exchanger. The dashed horizontal lines correspond to a capital cost (heat exchanger + heat engine) target of $1.2/W which assumes a capacity factor of 0.9. The kinks in the plot at various temperatures are due to changes in the heat exchanger /fluid combination on the hot side and cold side depending on the temperature based on the optimization algorithm (see SI and Table 1).

Figure 5: Cost of heat exchanger per unit electrical power output as a function of power for different values of relative Carnot efficiency (ϕ) and waste heat temperature (T_{source}). The dashed horizontal lines correspond to a capital cost (heat exchanger + heat engine) target of $1.2/W which assumes a capacity factor of 0.9. For T_{source} less than 100 °C, the cost of the heat exchanger itself is much higher than the target value for most values of power.

Figure 6: Allowable cost of heat engine. C_{he}, as a function of power output for different values of relative Carnot efficiency (ϕ) and waste heat temperature (T_{source}).

Figure 7: Minimum viable temperature as a function of capacity factor and different values of relative Carnot efficiency (ϕ) of the heat engine assuming a lifetime of 25 years and a discount rate of 6%**.** Note that for higher discount rate or lower lifetime the minimum viable temperature will increase as the allowed capital cost will be lower (Fig. 2). This curve was generated assuming that the cost of the heat engine (C_{he}) is $0.25/W which is the same as gas turbines (this is a highly optimistic assumption, see manuscript for details). For higher values of heat engine cost the curve will shift upwards and increase the minimum viable temperature. The minimum size of the heat engine for various conditions shown still varies between 100 kW – 1 MW.